Journal of Thermal Analysis and Calorimetry (2019) 137:65–77
https://doi.org/10.1007/s10973-018-7934-z

The synergistic effects of a novel intumescent flame-retardant poly-(4-nitrophenoxy)-phosphazene and ammonium polyphosphate on ABS systems

Yunyun Yang[1] · Hang Luo[1] · Xilei Cao[1] · Feng Zhou[1] · Weibo Kong[1] · Xufu Cai[1]

Received: 22 June 2018 / Accepted: 16 November 2018 / Published online: 28 November 2018

Abstract
Novel intumescent flame retardancy acrylonitrile–butadiene–styrene (ABS) composites were prepared by adding poly-(4-nitrophenoxy)-phosphazene (DPP) as charring and inflate agent, and ammonium polyphosphate (APP) as acid and inflate agent. The flame-retardant properties of samples were studied by LOI, UL-94 and microscale combustion calorimeter (MCC), when the ratio of APP and DPP was 1:1 with 30 mass% additive amount, the LOI was 27%, and the UL-94 reached V-0 rating. To further study the synergistic effects of DPP and APP, the charring-forming capability and thermal behavior of ABS composites were extensively studied by thermogravimetric analysis (TGA) under nitrogen and air, respectively. Also the binary system of APP and DPP was investigated by TGA measurements to identify their reaction and the synergistic mechanisms. The char residues were studied by X-ray photoelectron spectroscopy (XPS), scanning electron microscopy (SEM) analysis and Fourier transform infrared (FTIR). Meanwhile, the gaseous products generated in degradation process were detected by thermogravimetric analysis coupled Fourier transform infrared (TGA/FTIR).

Keywords Poly-(4-nitrophenoxy)-phosphazene (DPP) · Ammonium polyphosphate (APP) · Acrylonitrile–butadiene–Styrene (ABS) · Intumescent flame retardants (IFRs) · X-ray photoelectron spectroscopy (XPS)

Introduction

Acrylonitrile–butadiene–styrene (ABS), a widely used thermoplastic material [1, 2], is the most significant materials in 3D-printing field [3–6], because of its good mechanical properties, chemical resistance and processing advantages [7–9]. However, the combustibility and molten dripping is the odious shortcoming for ABS, which will limit its development and applications [10, 11]. To decrease the flammability of ABS, introducing flame retardant is the most convenient and economic technique [7, 8]. In order to resolve the problems of combustibility and molten dripping of ABS, intumescent flame retardants (IFRs) are selected as halogen-free agents for flame-retardant ABS [12–14]. Typically, the principal ingredients of IFRs are charring agents, inflate sources and acid sources. And a typical example is the ammonium polyphosphate (APP)/pentaerythritol (PER) system [15, 16]. However, PER, functioned as charring agent in this case, is small molecular compound and consists of hydroxyl groups, which will lead to a severe deterioration of the flame retardancy [17], and generates negative effect on the stability of composites in hygrothermal environment [13]. Therefore, it is urgent and crucial to discover novel intumescent flame retardants, which is high molecular compound without hydroxyl groups, applied in flame retardancy ABS.

As we known, phosphazenes with an alternating P-N backbone have a wide temperature range of thermal and chemical stabilities [18], which have been used as efficient intumescent flame-retardant additives for polymers [19]. In our previous work, we found that nitro compounds had the ability of char forming and anti-dripping [20, 21]; the synthesis of hexakis(4-nitrophenoxy) cyclotriphosphazene (HNTP) was designed to be used as charring agent in the PC composite and ABS composites. It suggested that the

✉ Xufu Cai
caixf2008@scu.edu.cn

[1] College of Polymer Science and Materials, The State Key Laboratory of Polymer Materials Engineering, Sichuan University, Chengdu 610065, China

introduction of nitro increased the percentage of nitrogen and the P-N synergism effects [22, 23]. Nevertheless, HNTP was a small molecular compound. To avoid the negative influence of small molecular compounds mentioned above, poly-(4-nitrophenoxy)-phosphazene (DPP), which possessed high molecular compounds without hydroxy groups, was designed to be used as charring agent and inflate agent. Meanwhile, ammonium polyphosphate (APP) was used as acid and inflate agent [24–26], which can indeed act either in the gas phase by inhibiting the flame and in the condensed phase by interacting with the polymeric matrix and promoting char [27, 28].

In this work, DPP, which possessed high molecular compounds without hydroxy groups, and APP, which also was high molecular compound, were mixed with ABS as intumescent flame retardants to decrease the combustibility of ABS. DPP was used as charring and inflate agent, and APP was used as acid and inflate agent. The flame-retardant properties of samples were studied by LOI, UL-94 and microscale combustion calorimeter (MCC). For qualitatively analyzing the synergistic effects of APP and DPP, thermogravimetric analysis (TGA) measurements were used to study the synergistic effects of DPP and APP, the char-forming capability and thermal behavior of ABS composites under nitrogen and air, respectively. Also the binary system of APP and DPP was investigated by TGA measurements to identify their reaction and the synergistic mechanisms. The char residues were studied by X-ray photoelectron spectroscopy (XPS), scanning electron microscopy (SEM) analysis and Fourier transform infrared (FTIR). At the same time, the gaseous products generated in degradation processing were detected by thermogravimetric analysis coupled Fourier transform infrared (TGA/FTIR).

Scheme 1 Structure of poly-(4-nitrophenoxy)-phosphazene (DPP)

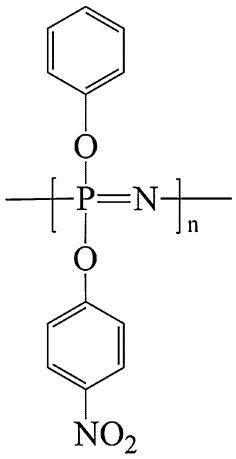

Table 1 Compositions of the investigated materials

Sample	Percentage of mass/%		
	ABS	DPP	APP
ABS-0	100	0	0
ABS-1	70	0	30
ABS-2	70	30	0
ABS-3	70	22.5	7.5
ABS-4	70	20	10
ABS-5	70	10	20
ABS-6	70	7.5	22.5
ABS-7	70	15	15

Experimental

Materials

Acrylonitrile–butadiene–styrene copolymer (0215A) used in this work was purchased from Jilin petrochemical company limited. Ammonium polyphosphate (APP) was obtained from Zhejiang Long you GD Chemical Industry Company. The APP ($n > 1000$) with branched chain was called crystalline phase II. Poly-(4-nitrophenoxy)-phosphazene ($n > 10$, DPP, showed in Scheme 1) was prepared in laboratory [29].

Samples preparation

ABS, DPP and APP were dried in a vacuum oven at 80 °C for 12 h prior to processing, respectively. According to a certain proportion of DPP, APP and ABS were added into a HAAKE plastic order mixer at 180 °C and 30 rpm for 4.5 min. The mixed samples were transferred to a mold and preheated at 180 °C for 8 min, then pressed at 15 MPa, and then cooled to room temperature while maintaining 5 MPa pressure to obtain the composite sheets for further measurements. In this work, the percentage of flame retardants was 30 mass%. The ratio of DPP to APP was noted in the Table 1.

Instrumentation

Flammability and stability of all samples were assessed by LOI, UL-94 vertical burning test, microscale combustion calorimeter (MCC) and thermogravimetric analysis (TGA). LOI was measured at room temperature on an oxygen index instrument (XYC-75) (Chende Jinjian Analysis Instrument Factory) according to the ASTM D2863-08 standard. UL-94 vertical burning tests were performed on a CZF-2 instrument (Jiangning Analysis Instrument Factory) according to UL-94 ASTM D635-77 standard. Pyrolysis combustion flow calorimetry experiments were carried out

Table 2 LOI and UL-94 test results of the ABS composites

Sample	LOI/ %	UL-94 (3.20 mm)						
		Rating	t_1/s	First dripping	t_2/s	Second dripping	Mass loss/%	Ignited
ABS-0	18 ± 1	No	56 ± 9	Yes	–	–	95 ± 5	Yes
ABS-1	23 ± 1	No	28 ± 9	Yes	–	No	84 ± 6	Yes
ABS-2	23 ± 1	V-2	12 ± 6	Yes	14 ± 5	No	29 ± 4	Yes
ABS-3	24 ± 1	V-1	14 ± 4	1 drop	10 ± 6	No	18 ± 5	No
ABS-4	24 ± 1	V-1	12 ± 5	Yes	13 ± 6	No	23 ± 7	No
ABS-5	25 ± 1	V-1	11 ± 5	Yes	14 ± 5	No	25 ± 6	No
ABS-6	25 ± 1	V-1	13 ± 4	Yes	13 ± 5	No	29 ± 3	No
ABS-7	27 ± 1	V-0	10 ± 6	No	8 ± 6	No	21 ± 5	No

on a FAA-PCFC microscale combustion calorimeter produced by Fire testing technology (FTT, UK). The flow was a stream of nitrogen and oxygen flowing at 80 mL min^{-1} with oxygen/nitrogen flow rate was set at 20/80, according to ASTM D7309-07 standard. All samples were tested in triplicate and the data obtained were reproducible to within ± 10%. The measurement of TGA was taken using a Netzsch TG209 F1 thermogravimeter at a linear heating rate of 10 °C min^{-1} within the temperature range from 30 to 800 °C under air or nitrogen flow of 60 mL min^{-1}. All the mass of samples was kept at 8.0 ± 0.5 mg. Also the binary system of APP and DPP was investigated by TGA measurements to identify their reaction and the synergistic mechanisms under air or nitrogen flow.

In order to go further study the synergy of APP and DPP, the surface combustion residues left by LOI (fully burned samples) were detected by X-ray photoelectron spectroscopy (XPS), scanning electron microscopy (SEM) analysis and Fourier transform infrared (FTIR), respectively. XPS was carried out with XSAM 800 spectrometer (Kratos Co., UK), using Al Ka excitation radiation (1486.6 eV), operated at 12 kV and 15 mA. Bing energies were referenced to the carbonaceous carbon at 285.0 eV.

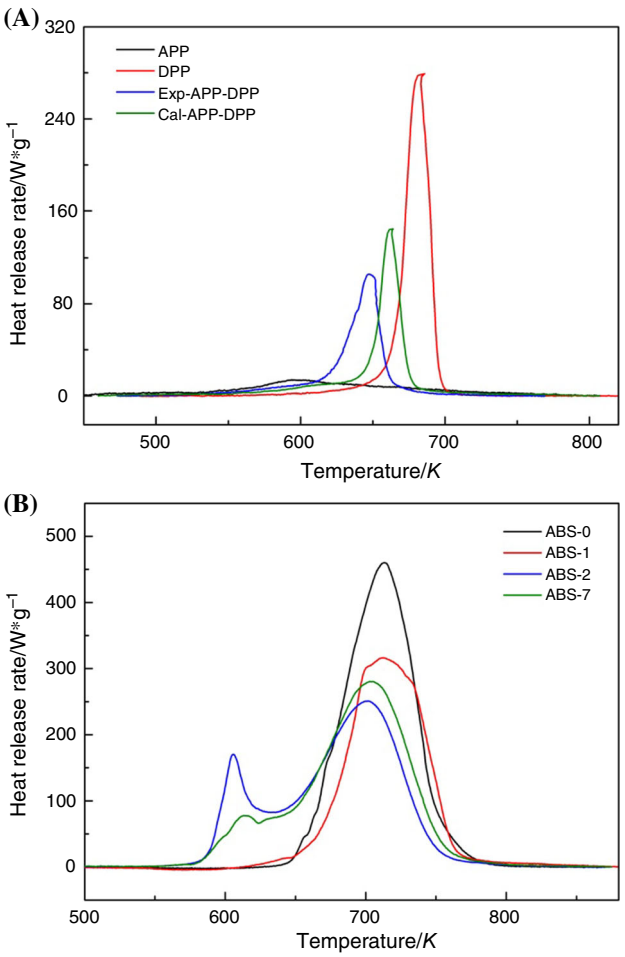

Fig. 1 MCC curves of composites and flame retardant, Exp-APP-DPP was the MCC results of binary system APP and DPP (the ratio of APP and DPP was 1:1), Cal-APP-DPP was the calculation results of binary system (was assumed by 50%APP + 50%DPP)

Table 3 MCC data of PC composites and flame retardant

Sample	PHRR ± 5 W/g	T_P ± 5 K	THR ± 0.5 KJ/g	HRC ± 10 J/g K
APP	14	594	1.88	307
DPP	279	686	4.09	266
Exp-APP-DPP[a]	106	647	3.28	112
Cal-APP-DPP[b]	140	686	3.51[c]	–
ABS-0	460	713	27.33	467
ABS-1	316	713	21.14	642
ABS-2	251	695	23.65	380
ABS-7	280	702	24.27	362

PHRR, the peak of heat release rate; Tp, temperature at peak heat release rate; THR, total heat released; HRC, heat release capacity

[a]Exp-APP-DPP: the MCC results of binary system APP and DPP (the ratio of APP and DPP was 1:1)

[b]Cal-APP-DPP: the calculation results of binary system(was assumed by 50%APP + 50%DPP)

[c]THR of Cal-APP-DPP was the integrate of MCC curves of Cal-APP-DPP

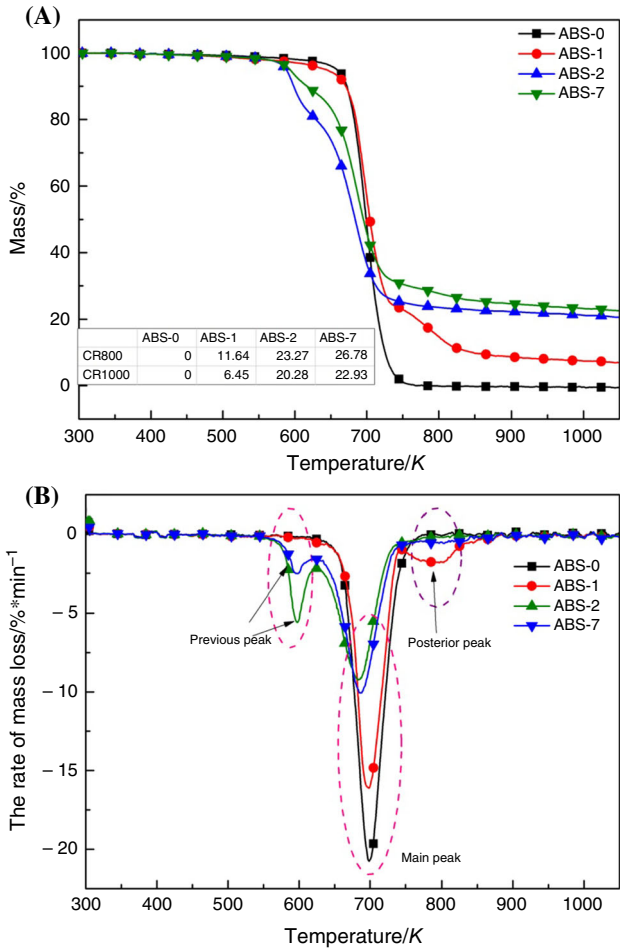

Fig. 2 TGA curves (**a**)(CR800 was the char residual yield at 800 K, CR1000 was the char residual yield at 1000 K) and DTG curves (**b**) of ABS-0, ABS-1, ABS-2 and ABS-7 under nitrogen

Samples for SEM (JeolJSM-7500F) were prepared by low-temperature fracturing and sputtered with gold on the surface prior to measurement. The char residues on the surface of the flame-retarded composites after LOI tests were characterized with an infrared spectrometer (Nicolet 50, Nicolette Co., USA) using KBr pellets.

And gaseous products generated in degradation were detected by thermogravimetric analysis coupled Fourier transform infrared (TGA/FTIR). TGA/FTIR measurements were taken on a Mettler Toledo TGA/DSC 1 STAR^e System thermogravimeter coupled with a Nicolet iS10 FTIR spectrophotometer. About 8.0 ± 0.2 mg of each sample was heated from 323 to 883 K with a heating rate of 10 K min^{-1} under air condition.

Results and discussion

The flammability properties of ABS composites samples

The LOI and UL-94 results of the samples are listed in Table 2. It showed that the addition of APP and DPP was beneficial to improve the flame retardancy of ABS. When APP and DPP were added alone, LOI was 23%, and UL-94 reached the V-2 rating. The addition of APP and DPP did not eliminate the molten drops of ABS at first fire test. However, the molten drops of blends disappeared at second fire test. APP and DPP were used as IFR system and added together to further improve the flame retardancy of ABS. To find the optimum proportion of APP and DPP, APP and DPP were added together as different ratio. According to the results of LOI and UL-94, when the ratio of APP and DPP was 1:1, the LOI of ABS-7 was 27%, and the UL-94 reached V-0 rating.

MCC has been suggested as a method to assess the flammability characteristics of mg-sized sample [30, 31]. Heat release rate (HRR) is calculated from the oxygen depletion measurements. Heat release capacity (HRC) is obtained by dividing the sum of the peak heat release rate (PHRR) by the heating rate. The total heat release (THR) is obtained by integrating the HRR curve. Figure 1 and

Table 4 TGA and DTG results of ABS-0, ABS-1, ABS-2 and ABS-7 under nitrogen

Sample	Temperature/K				Peak Rate/% min^{-1}			Residual yield/%	
	$T_{5\%}$	T_{Pre}	T_{Main}	T_{Pos}	P_{Pre}	P_{Main}	P_{Pos}	800 K	1000 K
ABS-0	658.4 ± 5	–	698.9 ± 7	–	–	− 21.2 ± 1	–	0	0
ABS-1	643.6 ± 5	–	697.9 ± 7.5	794.4 ± 8	–	− 15.8 ± 1	− 1.9 ± 0.2	14.7 ± 1	7.4 ± 0.5
ABS-2	587.9 ± 4	597.7 ± 4.5	683.5 ± 6.5	–	− 5.6 ± 1	− 9.3 ± 0.5	–	23.4 ± 2	21.3 ± 1
ABS-7	593.2 ± 4	597.8 ± 5	685.2 ± 6	–	− 2.5 ± 0.5	− 10.1 ± 0.7	–	27.8 ± 2	23.2 ± 1.5

$T_{5\%}$, the average temperature of 5% mass loss decomposition (set $T_{5\%}$ as initial decomposition temperature); T_{Pre}, the average temperature of the previous decomposition peak; T_{Main}, the average temperature of the main decomposition peak; T_{Pos}, the average temperature of the previous decomposition peak; Peak rate, the average mass loss rate at the decomposition peak; P_{Pre}, the average mass loss rate at the previous decomposition peak; P_{Main}, the average mass loss rate at the main decomposition peak; P_{Pos}, the average mass loss rate at the posterior decomposition peak; Residual yield, the average char residual yield at 800 K and 1000 K

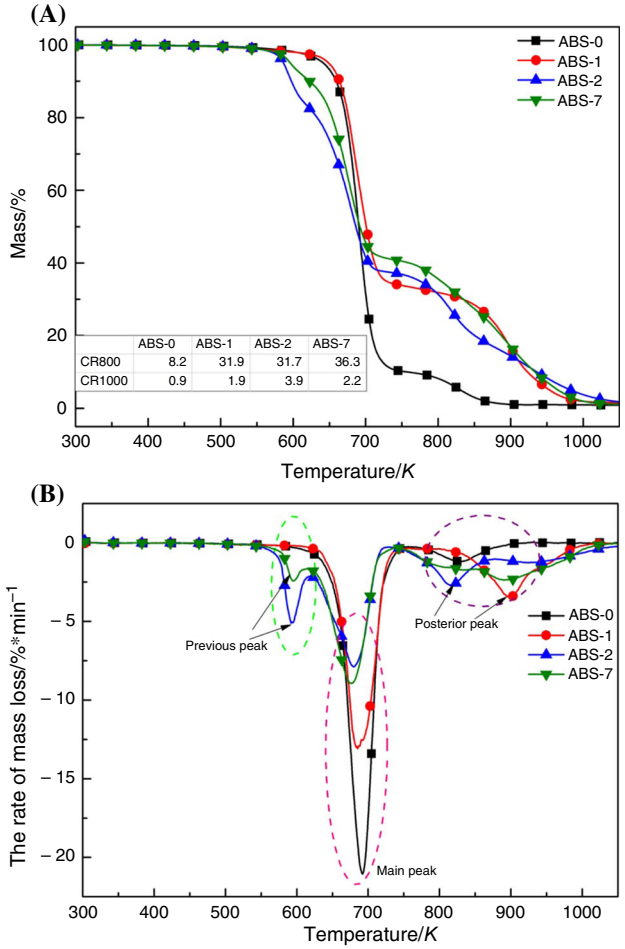

Fig. 3 TGA curves (**a**) (CR800 was the char residual yield at 800 K, CR1000 was the char residual yield at 1000 K) and DTG curves (**b**) of ABS-0, ABS-1, ABS-2 and ABS-3 under air

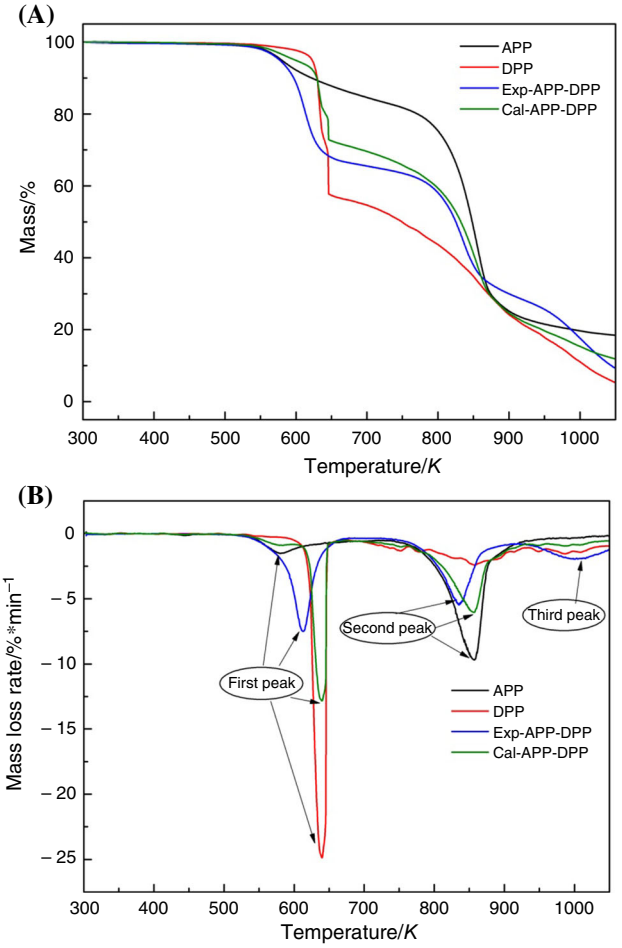

Fig. 4 TGA (**a**) and DTG (**b**) curves for APP + DPP (the ratio of APP:DPP was 1:1) binary system under air

Table 3 are the heat release rate curves and data from the MCC of flame retardant and samples, respectively. Exp-APP-DPP was the MCC results of binary system APP and DPP (the ratio of APP and DPP was 1:1). Cal-APP-DPP was the calculation results of binary system (was assumed by 50%APP + 50%DPP). In Fig. 1a, APP had lowest PHRR and THR with lowest decomposition temperature. The HRC of DPP was lower than that of APP. By contrast, the MCC curve of Exp-APP-DPP showed that the reaction between APP and DPP reduce the PHRR and THR.

Table 5 TGA and DTG results of ABS-0, ABS-1, ABS-2 and ABS-7 under nitrogen

Sample	Temperature/K				Peak Rate/% min^{-1}			Residual yield/%	
	$T_{5\%}$	T_{Pre}	T_{Main}	T_{Pos}	P_{Pre}	P_{Main}	P_{Pos}	800 K	1000 K
ABS-0	641.9 ± 5	–	692.3 ± 6	829.7 ± 6	–	− 21.1 ± 2	− 1.2 ± 0.2	8.2 ± 0.5	0.9 ± 0.1
ABS-1	649.1 ± 5	–	685.2 ± 5.5	898.7 ± 7	–	− 13.1 ± 1	− 3.5 ± 0.2	31.9 ± 1	1.9 ± 0.2
ABS-2	586.8 ± 3	592.3 ± 4	680.3 ± 5	815.3 ± 6	− 5.1 ± 1	− 7.9 ± 0.5	− 2.7 ± 0.1	31.7 ± 1	3.9 ± 0.2
ABS-7	596.3 ± 4	594.4 ± 4	676.2 ± 4.5	889.4 ± 7	− 2.4 ± 0.5	− 8.9 ± 0.5	− 2.3 ± 0.1	36.3 ± 1	2.2 ± 0.2

$T_{5\%}$, the average temperature of 5% mass loss decomposition(set $T_{5\ \%}$ as initial decomposition temperature); T_{Pre}, the average temperature of the previous decomposition peak; T_{Main}, the average temperature of the main decomposition peak; T_{Pos}, the average temperature of the previous decomposition peak; Peak rate, the average mass loss rate at the decomposition peak; P_{Pre}, the average mass loss rate at the previous decomposition peak; P_{Main}, the average mass loss rate at the main decomposition peak; P_{Pos}, the average mass loss rate at the posterior decomposition peak; Residual yield, the average char residual yield at 800 K and 1000 K

Table 6 TGA and DTG results of binary system under air

Sample	Temperature/K				Peak rate/% min^{-1}		
	$T_{5\%}$	T_{P1}	T_{P2}	T_{P3}	P_1	P_2	P_3
APP	579.6 ± 3	580.2 ± 3	857.3 ± 7	–	− 1.5 ± 0.5	− 9.7 ± 0.5	–
DPP	622.6 ± 6	638.8 ± 6	–	–	− 24.9 ± 0.7	–	–
Exp-APP-DPP	576.9 ± 3	613.1 ± 5	835.5 ± 5	1000.7 ± 10	− 7.5 ± 0.6	− 5.5 ± 0.4	− 1.9 ± 0.25
Cal-APP-DPP	598.9 ± 5	639.3 ± 5	856.9 ± 5	–	− 12.8 ± 0.75	− 5.9 ± 0.5	–

$T_{5\%}$, the average temperature of 5% mass loss decomposition(set $T_{5\ \%}$ as initial decomposition temperature); T_{P1}, the average temperature of the first decomposition peak; T_{P2}, the average temperature of the second decomposition peak; T_{P3}, the average temperature of the third decomposition peak; Peak rate, the average mass loss rate at the decomposition peak; P_1, the average mass loss rate at the first decomposition peak; P_2, the average mass loss rate at the second decomposition peak; P_3, the average mass loss rate at the third decomposition peak; Exp-APP-DPP, the TGA results of binary system APP and DPP (the ratio of APP and DPP was 1:1); Cal-APP-DPP, the calculation results of binary system(was assumed by 50%APP + 50%DPP)

There was about 45.4% reduction in PHRR with 30 mass% DPP, while was 31.3% reduction with 30 mass%APP, and 39.1% reduction with 15 mass% DPP and 15 mass% APP. But the tendency of HRC was different. There was about 18.6% reduction in HRC with 30 mass% DPP, while was 37.5% increase with 30 mass%APP, and 22.5% reduction with 15 mass% DPP and 15 mass% APP. And T_P of all ABS composites were at the same level in the error range. The addition of flame retardants made a decrease in THR. The results of samples confirmed that the introduction of DPP was beneficial to reduce PHRR, HRC and THR while the introduction of BDP was benefit of reducing PHRR, and THR.

The thermal decomposition behaviors under nitrogen

For qualitatively analyzing the synergistic effects of APP and DPP, TGA was used to study the mass loss and mass loss rate of samples under pure nitrogen is, respectively, presented in Fig. 2a and b. In order to simplify the curves, only the ABS sample with 1:1 ratio of APP and DPP was illustrated. With the addition of APP, the onset decomposition temperature of samples did not change very much. But the addition of DPP had shifted the onset decomposition temperature. The addition of APP and DPP increased the char residues of ABS. And the addition of APP and DPP changed the decomposition peak of ABS from one to two.

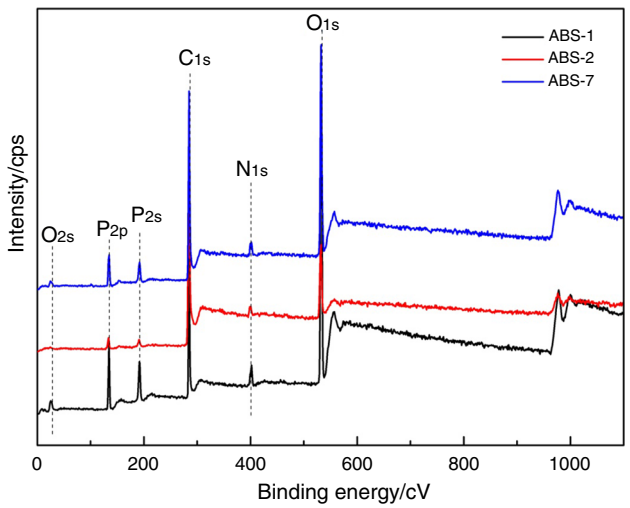

Fig. 5 Full-scan XPS spectra of ABS composites

Table 4 clearly lists the results got from the TGA measurements. The initial decomposition temperature of ABS-1 was close to that of ABS-0. But the addition of DPP shifted the initial decomposition temperature of ABS by 70.5 K. As shown in Fig. 2b, except for ABS-0, all the other samples showed two thermal decomposition steps. ABS-1 had a main decomposition peak which was associated with the decomposition of ABS, and a posterior decomposition peak which was related to the decomposition of APP. The main decomposition temperature of ABS-1 was same with that of ABS-0, but the rate of the main decomposition peak of ABS-1 was 74.5% of that of ABS-0. At the same time, the residual yield of ABS-1 increased from 0 to 14.7% at 800 K. It indicated that the addition of APP postponed the decomposition of ABS.

Different from the effect of APP, the addition of DPP shifted the initial decomposition temperature and main

Table 7 The XPS results of ABS composites

Sample	Atomic ratio/%				C/O[a]
	C1s	N1s	O1s	P2p	
ABS-1	43.57	4.925	41.63	9.88	1.05
ABS-2	82.33	2.281	13.07	2.324	6.30
ABS-7	60.27	3.987	29.46	6.285	2.05

[a]The ratio of C atom and O atom

decomposition temperature to low temperature by 70.5 K and 15.4 K, respectively. And the addition of DPP introduced a previous decomposition peak. The rate of main decomposition was decreased by 56.1%. And the residual yield of ABS-2 increased from 0 to 23.4% at 800 K, and from 0 to 21.3% at 1000 K. Those results implied that that the addition of DPP accelerated the decomposition of ABS. The variation of residual yield at high temperature showed the thermal stability of the product.

With the addition of APP and DPP, the initial decomposition temperature and main decomposition temperature were shifted to low temperature by 65.2 K and 13.7 K, respectively. The temperature of the previous peak of ABS-2 and ABS-7 was same. But the P_{Pre} of ABS-7 was 44.6% of that of ABS-2. The T_{Main} and P_{Main} of ABS-2 and ABS-7 were close. Meanwhile, the residual yield of ABS-7 increased from 0 to 27.8% at 800 K, and from 0 to 23.2% at 1000 K. Those results showed the synergistic effects of APP and DPP.

The thermal decomposition behaviors under air

The decomposition of ABS samples under air atmosphere was also detected by TGA analysis. The TGA results of APP and DPP mixed ABS under air are presented in Fig. 3. The participation of air weakened the char residual yield of all samples. The char residual yield of ABS-1, ABS-2 and ABS-7 still was higher than the yield of pure ABS.

Table 5 summarizes the main parameters of TGA measurements under air. The participation of oxygen shifted the $T_{5\%}$ of ABS-0 to low temperature by 16.5 K, while $T_{5\%}$ of other samples was shifted to high temperature or did not change. The obvious influence of the oxygen on the decomposition behaviors of ABS-0 samples was decomposition steps. There were two decomposition steps. One was same with the main decomposition peak under nitrogen; the other was a posterior peak at 829.7 K with a low mass loss rate.

Compared with ABS-0, the $T_{5\%}$ and the temperature at main decomposition peak of ABS-1 were shifted to low temperature about 10 K, the temperature at posterior peak shifted to high temperature by 69 K. There was also difference in the rate of decomposition. The addition of APP made the P_{Main} of ABS-1 to be 62.1% of the P_{Main} of ABS-0, but the P_{Pos} of ABS-1 was 2.9 times of that of ABS-0. The char residual yield of ABS-1 increased from 8.2 to 31.9% at 800 K and from 0.9 to 1.9% at 1000 K.

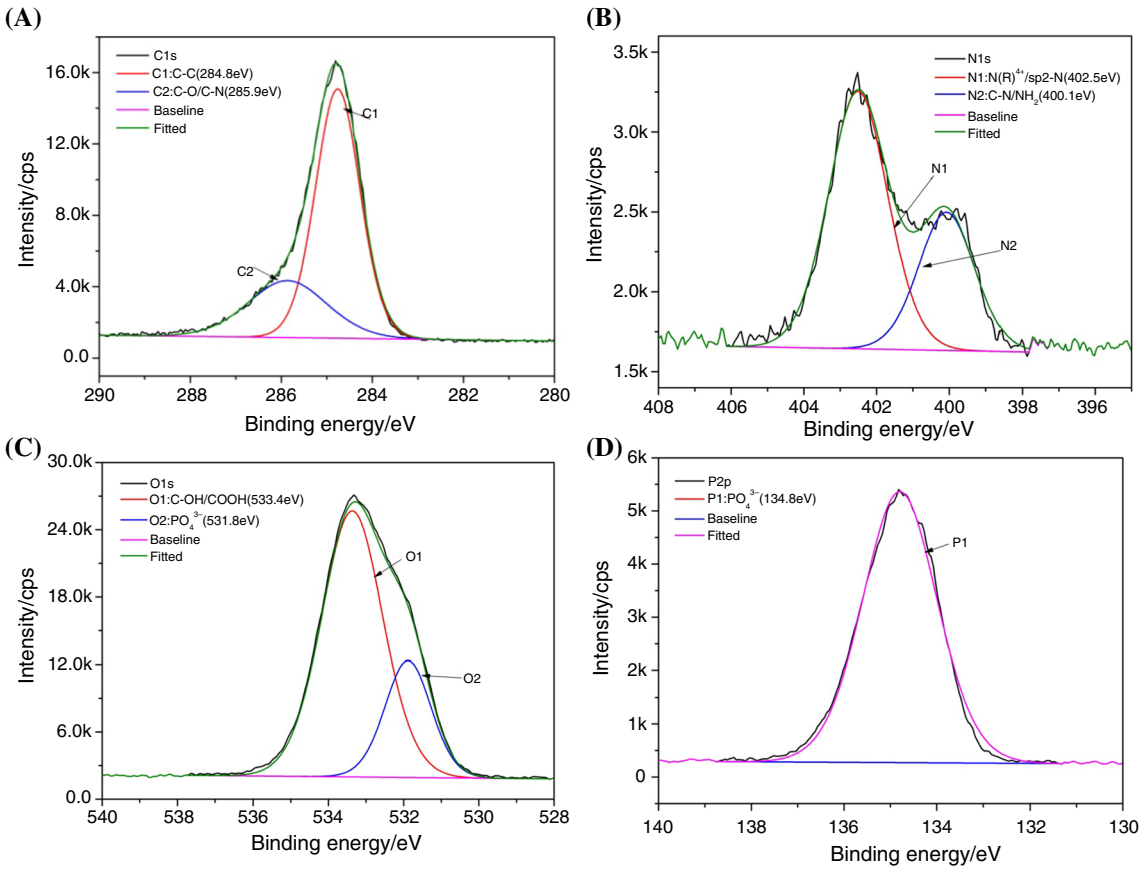

Fig. 6 C1 s (**a**), O1 s (**b**), N1 s (**c**), and P2p (**d**) XPS spectra of ABS-1

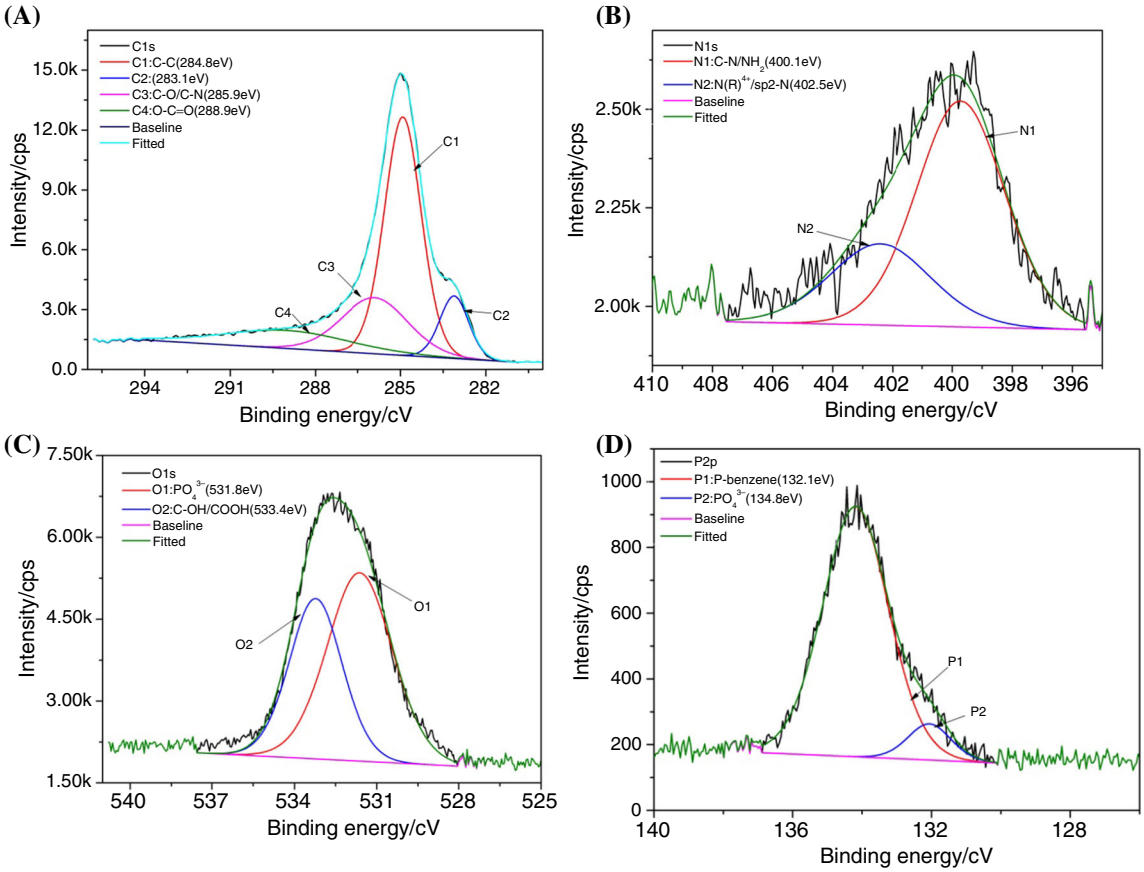

Fig. 7 C1s(**a**), O1s(**b**), N1s (**c**), and P2p (**d**) XPS spectra of ABS-2

With the addition of DPP, there were three decomposition peaks in the whole heating range. The $T_{5\%}$, T_{Main} and T_{Pos} were shifted to low temperature. But the rate at main decomposition was 37.4% of that of ABS-0. The residual yield of ABS-2 was 3.9 times of that of pure ABS at 800 K.

When APP and DPP were added together, the $T_{5\%}$, T_{Main} and T_{Pre} were similar to those of ABS-2, and the T_{Pos} was close to the T_{Pos} of ABS-1. Those similarities implied the influence of APP and DPP on ABS decomposition. The decrease in P_{Pre} and P_{Pos} and the increase in residual yield at 800 K suggested the synergistic effects between APP and DPP.

TGA analysis of binary system APP + DPP under air

In order to identify the reaction and the synergistic mechanisms between APP and DPP, the binary system was investigated; the ratio of APP:DPP was 1:1. In Fig. 4 and Table 6 the thermal analysis of APP and DPP binary system under air was presented. The mass loss of all samples occurred at about 550 K, while the process of APP and Exp-APP-DPP was earlier. DPP had one decomposition peak at 638.8 K in the rate of 24.9% min^{-1}, APP and Cal-APP-DPP had two decomposition peaks, and Exp-APP-DPP had three decomposition peaks. APP and DPP binary system demonstrated a lower thermal stability than the calculated binary system. The decomposition process of Exp-APP-DPP shifted to low temperature. $T_{5\%}$, T_{P1} and T_{P2} were reduced by 23, 26 and 21 K, respectively. These differences indicated that the reaction of APP and DPP shifts the decomposition of binary system to lower temperature.

The study of char residues by XPS, SEM and FTIR

To further study the synergistic effects of APP and DPP in remnant char, the chemical constitution of the charring residue of ABS-1, ABS-2 and ABS-7 left was investigated by XPS. Figure 5 presents the full-scan XPS spectra of ABS composites. To compensate for sample charging, all binding energies were referenced to C1 s at 285 eV. The peaks of carbon, oxygen, nitrogen and phosphorus were detected from the full-scanned XPS spectrum of ABS composites. The detailed data are presented in Table 7. As shown in Table 7, the addition of APP increased the atomic ratio of N1s, O1s and P2p, and the addition of DPP increased the atomic ratio of C1s. With the addition of

DPP, the C/O ratio of ABS-2 was 6 times of that of ABS-1, suggesting the charring ability of DPP.

The C1s, O1s, N1s and P2p spectra of ABS-1, ABS-2 and ABS-7 are shown in Figs. 6–8, respectively. The analysis of C1 s spectra showed that the addition of APP makes the C1 s spectra of ABS-1 have two peaks, 284.8 and 285.9 eV, which were belong to C–C (70.4%) and O–C=O (29.6%) bond, respectively [32, 33], while the C1 s spectra of ABS-2 had four peaks, 283.1, 284.8, 285.9 and 288.9 eV [34], which may belong to conjugation (10.8%), C–C (53.1%), C–O/C–N (22.5%), and O–C=O (13.6%) bond, respectively. There was a new peak of C–O/C–N, and the percentage of O–C=O bond was lower than that of ABS-1. Those results implied the charring ability of DPP. When APP and DPP were added together, the C1 s spectra of ABS-7 had three peaks, 248.8, 285.9 and 288.9 eV, which were belong to C–C (65.2%), C–O/C–N (30.3%) and O–C=O (4.5%) bond, respectively. With the addition of APP and DPP, the percentage of O–C=O decreased obviously. The N1s, O1s and P2p spectra of ABS-1 suggested the dehydration and salt-forming process of APP during heating. The comparison of O1s and P2p spectra indicated the reaction between ABS and DPP in heating.

Then the microcosmic morphology of the char heated by Muffle furnace was also investigated with SEM. Figure 9 presents the SEM micrographs of ABS composites char residues. According to Fig. 9 ABS-0, for pure ABS, the residues had poor chars on the surface of melting ABS. This defective char cannot insulate combustion-supporting gas and heat effectively, and cannot protect ABS from degrading during combustion. Therefore, in vertical burning tests, ABS burned off with molten dripping. As illustrated in Fig. 9 ABS-1, there were some char residues on the surface of ABS-1, which was consisted with the result of Fig. 3. Figure 9 ABS-2 shows the section and surface of ABS-2; its residues were intumescent and porous. This special structure was capable of preventing heat transfer, and protecting the polymer materials from further burning. In addition, this char structure can offer a useful shield to prevent melted ABS from dripping. As shown in Fig. 9 ABS-7, with the addition of APP and DPP, this char structure was same as the char structure of ABS-2. The surface of char residues and porous (inside of char residues) was look like the surface of ABS-1. Figure 10 lists the FTIR of char residues changed with the addition of APP and DPP. Also those results were consisted with the result of XPS.

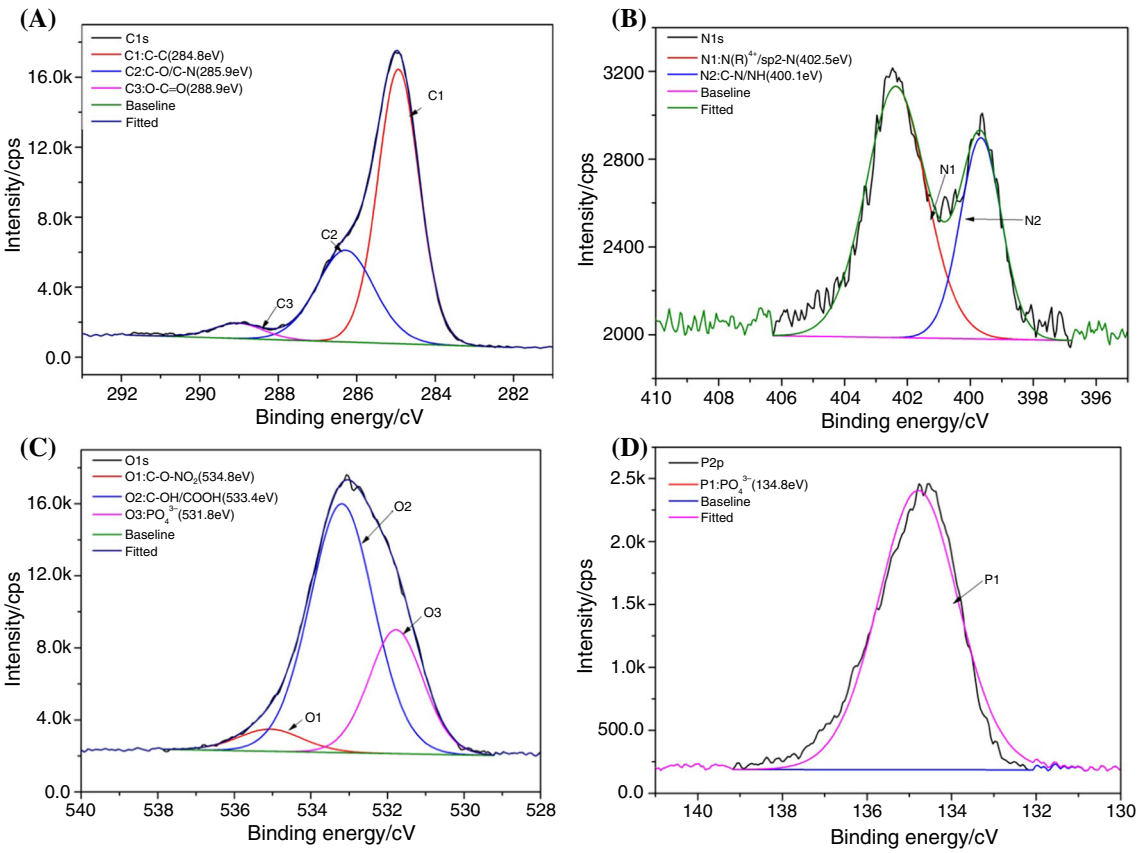

Fig. 8 C1s(**a**), O1s(**B**), N1s (**c**), and P2p (**d**) XPS spectra of ABS-7

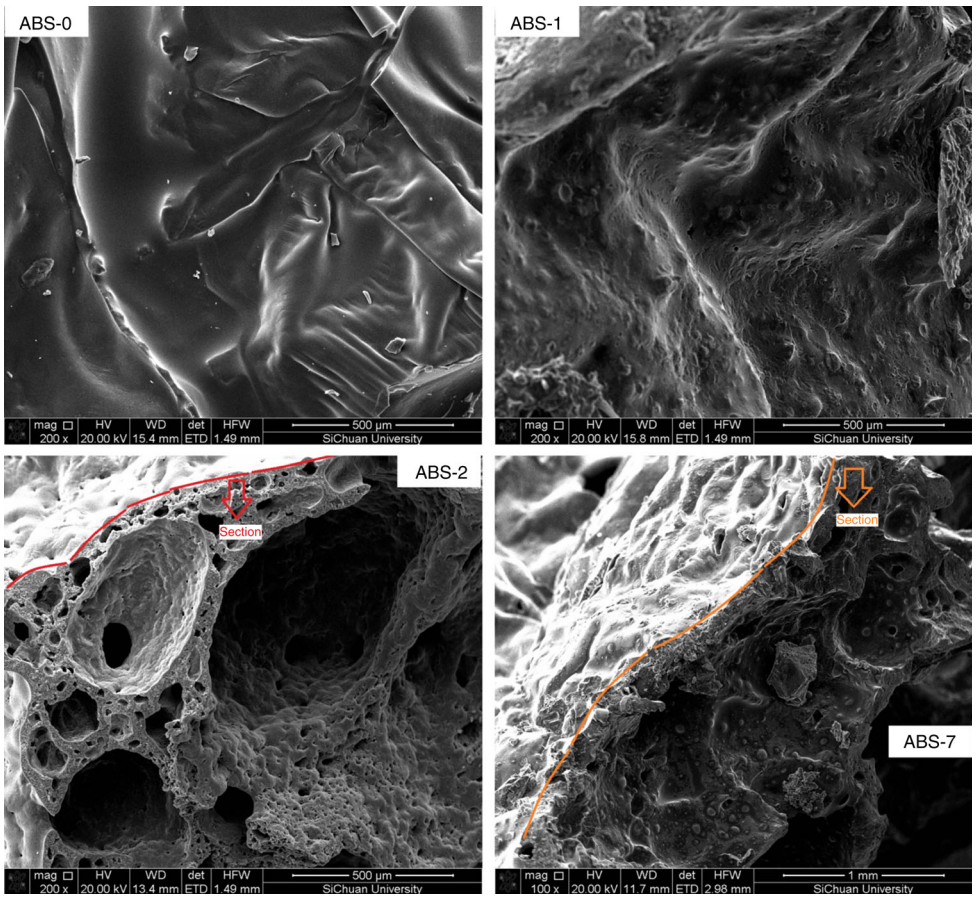

Fig. 9 SEM micrographs of char residues

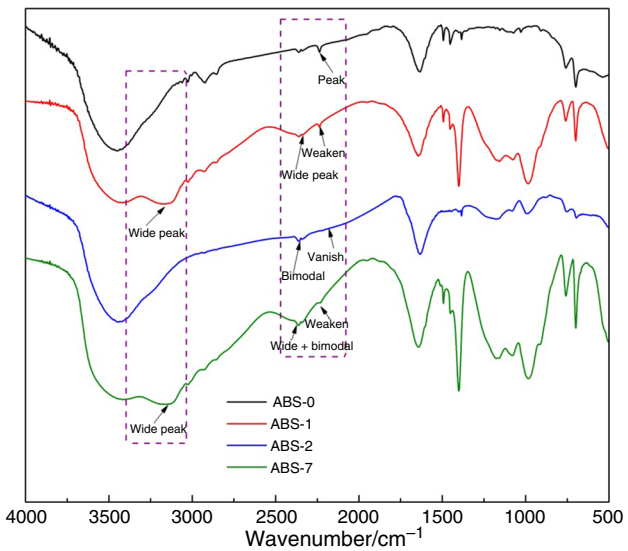

Fig. 10 FTIR of char residues

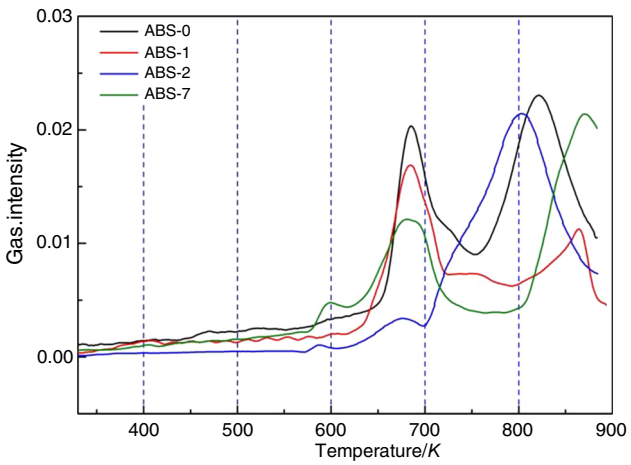

Fig. 11 Intensity of pyrolysis gaseous of ABS-0, ABS-1, ABS-2 and ABS-7

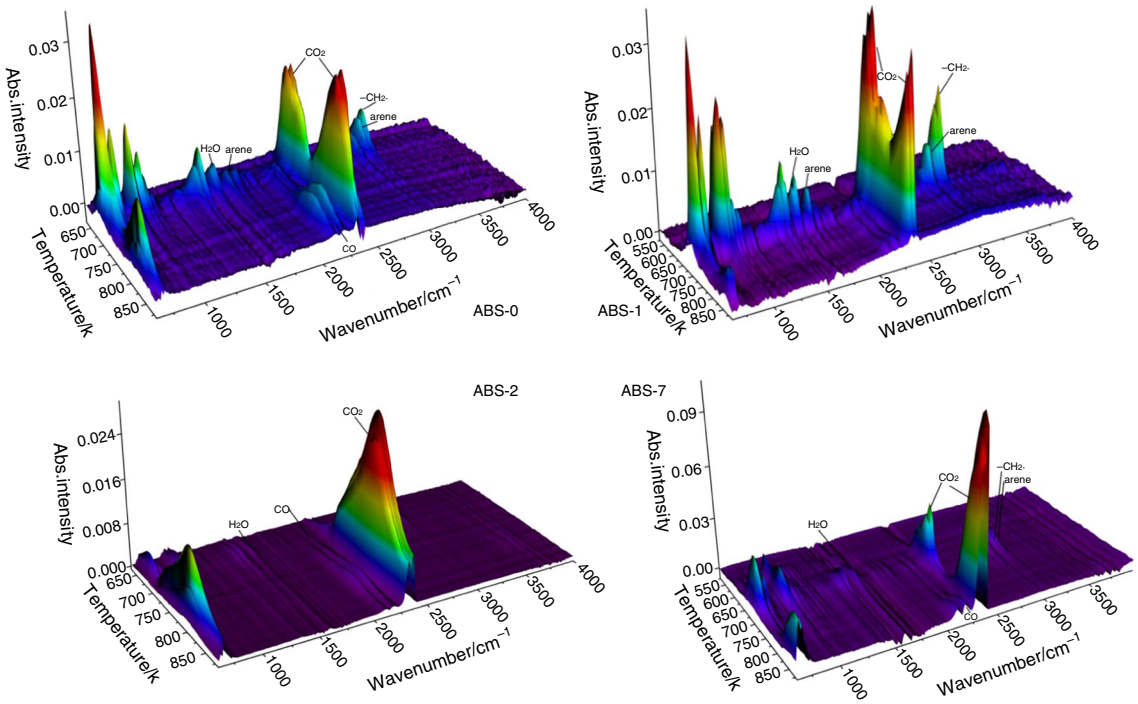

Fig. 12 Three-dimensional TGA/FTIR spectra of ABS-0, ABS-1, ABS-2 and ABS-7

The study of gaseous products

After TGA, XPS, FTIR and SEM analysis of char residues, the gaseous products generated in degradation processing were detected by TGA/FTIR. As shown in Fig. 11, the intensity of pyrolysis gaseous of ABS composites changed with the addition of flame retardant. Those different curves of gaseous intensity implied the different decomposition process.

Figure 12 shows the three-dimensional FTIR spectra of gaseous products of the composites at sharp losing mass temperature (600–880 K), respectively. For ABS-0, the generation of CO_2 and H_2O was observed over the whole range. But their peaks intensity increased with the rise of temperature firstly then decreased gradually after the first degradation peak. At the second peak, the trend of the intensity of CO_2 was same. Furthermore, in the temperature range of 630–750 K, there were the peaks of arene and alkane (in the range of 3100–2900 cm^{-1} and 1500–1630 cm^{-1}). With the addition of APP, the kind of peaks did not change. But the intensity of $–CH_2–$, arene, CO_2 and H_2O of ABS-1 was higher than that of ABS-0. And the intensity of CO of ABS-1 was lower than that of ABS-0. As showed in the XPS spectra of ABS-1, there was PO_4^{3-} in the char residues. And the heat release of ABS-1 was lower than that of ABS-0. It suggested that the formation of phosphate by APP dehydration absorbed part of the heat and changed the combustion behaviors of ABS.

For ABS-2, no new peaks or peak shifts were observed at each temperature. And in the main degradation temperature range, the main gaseous products of the ABS-2 were CO_2 and H_2O. However, the intensity of all absorbance peaks was weaker compared with ABS-0. The char residues yield coupled with the onset decomposition temperature results (Figs. 2, 3) indicated that the introduction of DPP accelerated the decomposition and catalyzed the production of stable materials during the decomposition process. So the gaseous products of the ABS-2 were less than that of ABS-1.

With the addition of APP and DPP, the intensity of CO_2 of ABS-7 was 3.87 times of that of ASB-0. The intensity of $–CH_2–$ and arene of ABS-7 was a half of that of ASB-0. The intensity of H_2O of ABS-7 was same as that of ABS-1. It indicated that the combustion of ABS was reduced by APP and DPP. These differences also indicated the synergistic effect of APP and DPP.

Conclusions

In this work, poly-(4-nitrophenoxy)-phosphazene(DPP) and ammonium polyphosphate (APP) were mixed with ABS as intumescent flame retardants to decrease the combustibility of ABS. When the ratio of APP and DPP was 1:1 with 30 mass% additive amount, the LOI of ABS-7 was 27%, and the UL-94 reached V-0 rating. With the addition of APP and DPP, the PHRR of ABS-7 was

reduced by 39.1%, and the HRC became 77.5% of that of ABS-0. TGA measurements were used to study the synergistic effects of APP and DPP under pure nitrogen and air, respectively. Under nitrogen, the residual yield of ABS-7 increased from 0 to 27.8% at 800 K, and from 0 to 23.2% at 1000 K. Under air, the residual yield of ABS-7 was 4.4 times of that of ABS-0 at 800 K, and 2.4 times at 1000 K. There were interactions between APP and DPP investigated by TGA measurements to identify their reaction and the synergistic mechanisms. The char residues were studied by XPS, SEM and FTIR. The results of XPS showed that the addition of APP increased the atomic ratio of N1s, O1s and P2p, the addition of DPP increased the atomic ratio of C1s. For ABS-7, the percentage of O–C=O decrease obviously, which meant more cross-linking formed with the addition of both APP and DPP. At the same time, the gaseous products generated in degradation process were detected by TGA/FTIR. The intensity of pyrolysis gaseous of ABS composites changed with the addition of flame retardant. All results suggested the synergistic effects between APP and DPP in gaseous process.

Acknowledgements We would like to thank the generous supports by the following: the Experiment center of Polymer science and engineering academy, Sichuan University.

References

1. Hart KR, Wetzel ED. Fracture behavior of additively manufactured acrylonitrile butadiene styrene (ABS) materials. Eng Fract Mech. 2017;177:1–13.
2. Zhang K, Gao F, Xu J, Wang L, Zhang Q, Kong J. Fabrication and dielectric properties of Ba0.6Sr0.4TiO3/acrylonitrile–butadiene–styrene resin composites. J Mater Sci Mater Electron. 2017;28:8960–8.
3. Clark B, Zhang Z, Christopher G, Pantoya ML. 3D processing and characterization of acrylonitrile butadiene styrene (ABS) energetic thin films. J Mater Sci. 2017;52:993–1004.
4. Wang X, Jiang M, Zhou Z, Gou J, Hui D. 3D printing of polymer matrix composites: a review and prospective. Compos B Eng. 2017;110:442–58.
5. Torrado AR, Shemelya CM, English JD, Lin Y, Wicker RB, Roberson DA. Characterizing the effect of additives to ABS on the mechanical property anisotropy of specimens fabricated by material extrusion 3D printing. Addit Manuf. 2015;6:16–29.
6. Dawoud M, Taha I, Ebeid SJ. Mechanical behaviour of ABS: an experimental study using FDM and injection moulding techniques. J Manuf Process. 2016;21:39–45.
7. Ozcelik B, Ozbay A, Demirbas E. Influence of injection parameters and mold materials on mechanical properties of ABS in plastic injection molding. Int Commun Heat Mass Transf. 2010;37:1359–65.
8. Kamelian FS, Saljoughi E, Shojaee Nasirabadi P, Mousavi SM. Modifications and research potentials of acrylonitrile/butadiene/styrene (ABS) membranes: a review. Polym Compos. 2017;39:2835–46.
9. Weng Z, Wang J, Senthil T, Wu L. Mechanical and thermal properties of ABS/montmorillonite nanocomposites for fused deposition modeling 3D printing. Mater Des. 2016;102:276–83.
10. Jian R, Chen L, Chen S, Long J, Wang Y. A novel flame-retardant acrylonitrile-butadiene-styrene system based on aluminum isobutylphosphinate and red phosphorus: flame retardance, thermal degradation and pyrolysis behavior. Polym Degrad Stab. 2014;109:184–93.
11. Zheng Z, Yang T, Wang B, Qu B, Wang H. Microencapsulated melamine phosphate via the sol–gel method and its application in halogen-free and intumescent flame-retarding acrylonitrile-butadiene-styrene copolymer. Polym Int. 2015;64:1275–88.
12. Zheng Z, Yang T, Wang B, Qu B, Wang H. Microencapsulated melamine phosphate via the sol–gel method and its application in halogen-free and intumescent flame-retarding acrylonitrile-butadiene-styrene copolymer. Polym Int. 2015;64:1275–88.
13. Zhang Y, Chen X, Fang Z. Synergistic effects of expandable graphite and ammonium polyphosphate with a new carbon source derived from biomass in flame retardant ABS. J Appl Polym Sci. 2013;128:2424–32.
14. Yin H, Yuan D, Cai X. Red phosphorus acts as second acid source to form a novel intumescent-contractive flame-retardant system on ABS. J Therm Anal Calorim. 2013;111:499–506.
15. Alongi J, Han Z, Intumescence Bourbigot S. Tradition versus novelty. A comprehensive review. Prog Polym Sci. 2015;51:28–73.
16. Tang Q, Wang B, Tang G, Shi Y, Qian X, Yu B, et al. Preparation of microcapsulated ammonium polyphosphate, pentaerythritol with glycidyl methacrylate, butyl methacrylate and their synergistic flame-retardancy for ethylene vinyl acetate copolymer. Polym Adv Technol. 2014;25:73–82.
17. Wang Y, Xu M, Li B. Synthesis of *N*-methyl triazine-ethylenediamine copolymer charring foaming agent and its enhancement on flame retardancy and water resistance for polypropylene composites. Polym Degrad Stab. 2016;131:20–9.
18. Zhou L, Zhang G, Li J, Zhao L, Zhang X, Wei X. Synthesis and characterization of polyphenylaminophosphazene and fluorinated polyarylaminophosphazene. J Appl Polym Sci. 2015. https://doi.org/10.1002/app.42542.
19. Nguyen TD, Chang S, Condon B, Uchimiya M, Fortier C. Development of an environmentally friendly halogen-free phosphorus-nitrogen bond flame retardant for cotton fabrics. Polym Adv Technol. 2012;23:1555–63.
20. Cao X, Yang Y, Luo H, Cai X. High efficiency intumescent flame retardancy between Hexakis (4-nitrophenoxy) cyclotriphosphazene and ammonium polyphosphate on ABS. Polym Degrad Stab. 2017;143:259–65.
21. Yang Y, Luo H, Cao X, Kong W, Cai X. Preparation and characterization of a water resistance flame retardant and its enhancement on charring—forming for polycarbonate. J Therm Anal Calorim. 2017;129:809–20.
22. Ma T, Guo C. Synergistic effect between melamine cyanurate and a novel flame retardant curing agent containing a caged bicyclic phosphate on flame retardancy and thermal behavior of epoxy resins. J Anal Appl Pyrol. 2017;124:239–46.
23. Mathew D, Nair CPR, Ninan KN. Phosphazene–triazine cyclomatrix network polymers: some aspects of synthesis, thermal- and flame-retardant characteristics. Polym Int. 2000;49:48–56.
24. Yao W, Wang H, Guan D, Fu T, Zhang T, Dou Y. The effect of soluble ammonium polyphosphate on the properties of water blown semirigid polyurethane foams. Adv Mater Sci Eng. 2017;2017:1–7.
25. Rajaei M, Wang D, Bhattacharyya D. Combined effects of ammonium polyphosphate and talc on the fire and mechanical properties of epoxy/glass fabric composites. Compos B Eng. 2017;113:381–90.
26. Wang W, Chen X, Gu Y, et al. Synergistic fire safety effect between nano-CuO and ammonium polyphosphate in

thermoplastic polyurethane elastomer. J Therm Anal Calorim. 2018;131(3):3175–83.
27. Ke C, Li J, Fang K, Zhu Q, Zhu J, Yan Q, et al. Synergistic effect between a novel hyperbranched charring agent and ammonium polyphosphate on the flame retardant and anti-dripping properties of polylactide. Polym Degrad Stab. 2010;95:763–70.
28. Zheng Z, Qiang L, Yang T, Wang B, Cui X, Wang H. Preparation of microencapsulated ammonium polyphosphate with carbon source- and blowing agent-containing shell and its flame retardance in polypropylene. J Polym Res. 2014; 21:443–47.
29. Xufu C, Yunyun Y, Xilei C, et al. The synthesis preparation of Poly-(4-nitrophenoxy)-phosphazene: CN, CN104974350A. 2015.
30. Shi Y, Kashiwagi T, Walters RN, Gilman JW, Lyon RE, Sogah DY. Ethylene vinyl acetate/layered silicate nanocomposites prepared by a surfactant-free method: enhanced flame retardant and mechanical properties. Polymer. 2009;50:3478–87.
31. Schartel B, Pawlowski KH, Lyon RE. Pyrolysis combustion flow calorimeter: A tool to assess flame retarded PC/ABS materials? Thermochim Acta. 2007;462:1–14.
32. Zhao H, Liu B, Wang X, Chen L, Wang X, Wang Y. A flame-retardant-free and thermo-cross-linkable copolyester: flame-retardant and anti-dripping mode of action. Polymer. 2014;55:2394–403.
33. Ke C, Li J, Fang K, Zhu Q, Zhu J, Yan Q, et al. Synergistic effect between a novel hyperbranched charring agent and ammonium polyphosphate on the flame retardant and anti-dripping properties of polylactide. Polym Degrad Stab. 2010;95:763–70.
34. Tabačiarová J, Mičušík M, Fedorko P, Omastová M. Study of polypyrrole aging by XPS, FTIR and conductivity measurements. Polym Degrad Stab. 2015;120:392–401.